DOI: 10.1002/chem.200701080

Supramolecular Helical Columns from the Self-Assembly of Chiral Rods

Ja-Hyoung Ryu, Lijun Tang, Eunji Lee, Ho-Joong Kim, and Myongsoo Lee*[a]

Abstract: Chiral-bridged rod molecules (CBRs) that consisted of bis(penta-*p*-phenylene) conjugated to an opened or closed chiral bridging group as a rigid segment and oligoether dendrons as flexible segments were synthesized and characterized. In the bulk state, both molecules self-assemble into a hexagonal columnar structure, as confirmed by X-ray scatterings and transmission electron microscopy (TEM) observations. Interestingly, these structures display opposite Cotton effects in the chromophore of the aromatic unit in spite of the same chirality (*R*,*R*) of the chiral bridging groups. The molecules were observed to self-assemble into cylindrical micellar aggregates in aqueous solution, as confirmed by light scattering and TEM investigations, and exhibit intense signals in the circular dichroism (CD) spectra, which are indicative of one-handed helical conformations. The CD spectra of each molecule showed opposite signals to each other, which were similar to those in the bulk. Notably, when the opened CBR was added to a solution of closed CBRs up to a certain concentration, the CD signal of the closed CBR was amplified. This implies that both molecules co-assemble into a one-handed helical structure because the opened chiral bridge is conformationally flexible, which is inverted to co-assemble with the closed CBR. These results demonstrate that small structural modifications of the chiral moiety can transfer the chiral information to a supramolecular assembly in the opposite way.

Keywords: chirality · helical columns · helical inversion · self-assembly · supramolecular chemistry

Introduction

Controlled self-assembly of elaborately designed molecules is a challenging topic for interdisciplinary research in the fields of chemistry, biology, and materials science because it provides the spontaneous generation of a well-defined, discrete supramolecular architecture from molecular components under thermodynamic equilibrium.[1] Precise control of molecular arrangements at the supramolecular level is essential to get well-defined nanoscopic architectures with specific shape and novel functionalities.[2] In particular, there is growing interest in the design of synthetic molecules that are able to self-assemble into compact helical aggregates, which are analogous to the DNA double helix and the collagen triple helix. Artificial helical architectures in synthetic self-assembling systems have been achieved with amplified supramolecular chirality by a variety of strategies, which include hydrogen bonding,[3,4] π–π stacking,[5–7] solvophobic effects,[8] and metal–ligand interactions.[9] Moreover, the control of helical sense induced by transfer of chiral information from the molecular to the supramolecular level, molecular recognition, and external stimuli has received increasing attention in biomimetic and synthetic supramolecular systems.[10–12] For example, the incorporation of chiral moieties in self-assembling organic molecules can induce chiral supramolecular assemblies and the configuration of the chiral moiety can decide the handedness of supramolecular helices.[13] Stupp et al. reported the mirror image of supramolecular helices.[14] They synthesized enantiomers of dendron–rod–coils attached to a chiral chain and showed that each molecule has the opposite Cotton effects depending on its chiral configuration, that is, the *R* or *S* form. Dendron–rod–coil nanostructures were imaged by atomic force microscopy, which showed one-dimensional helical nanostructures that were mirror images of each other. Meijer and co-workers also reported a helical structure obtained by the self-assembly of well-designed molecules.[1c,15] They have studied a variety of π-conjugated systems in which the individual π-conjugated molecules that contain a side-chain stereocenter form a one-handed helical structure that is dependent on the solvent polarity or temperature. Recently, we have

[a] Dr. J.-H. Ryu, Dr. L. Tang, E. Lee, H.-J. Kim, Prof. M. Lee
Center for Supramolecular Nano-Assembly
and Department of Chemistry
Yonsei University, Shinchon 134
Seoul 120-749 (Republic of Korea)
Fax: (+82) 2-393-6096
E-mail: mslee@yonsei.ac.kr

Supporting information for this article is available on the WWW under http://www.chemeurj.org/ or from the author.

shown that incorporation of a conjugated rod into an amphiphilic dumbbell-shaped molecular architecture gives rise to the formation of a helical nanostructure.[16] We have also shown the reversible transformation of the self-assembled structures of a dumbbell-shaped molecule between helical strands and nanocages triggered by the addition of aromatic guest molecules.[17]

Columnar assemblies formed from self-assembly of the organic molecules that contain rigid aromatic rods have been explored widely in liquid-crystalline and dilute solution states. Introduction of chirality into the side chains of the rod building blocks induces helical stacked arrays and molecular chirality is transferred to the central aromatic core, and is subsequently amplified through the formation of supramolecular helical columns.[13,15] However, incorporation of chiral segments into the center of rod building blocks, which have a significant influence on the supramolecular chirality owing to closer proximity to self-assembling units, remains challenging.[15e] To this end, we synthesized chiral-bridged rod molecules (CBRs) that contained the chiral groups in the center of rod building blocks and investigated their self-assembling behavior in both bulk and solution states by a combination of polarized optical microscopy, differential scanning calorimetry (DSC), circular dichroism (CD), transmission electron microscopy (TEM), dynamic light scattering (DLS), and powder X-ray diffraction measurements. As both molecules are based on an identical chiral configuration (*R*,*R*), the supramolecular chirality can mainly be attributed to the molecular architecture of the chiral groups in the center of the molecules, that is, opened or closed forms. Note that the opened chiral-bridged rod molecule (O-CBR) is able to freely rotate along the C*–C* bond in the chiral bridge. However, bond rotation in the closed chiral-bridged rod molecule (C-CBR) is hindered as a result of ring closure.

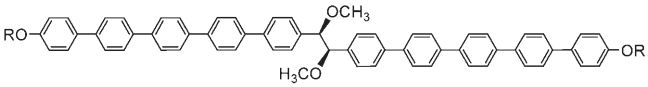

opened chiral bridge

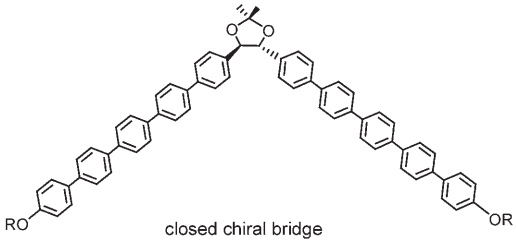

closed chiral bridge

Results and Discussion

Synthesis: The synthesis of CBRs that consist of bis(penta-*p*-phenylene) conjugated to a chiral moiety as the rigid segment and oligoether dendrons as the flexible segment is outlined in Scheme 1 and begins with the preparation of aromatic scaffolds and an oligoether dendron according to previously described procedures.[18,19] Compound (*R*,*R*)-**4**, which is based on an opened chiral group, and (*R*,*R*)-**5**, which is

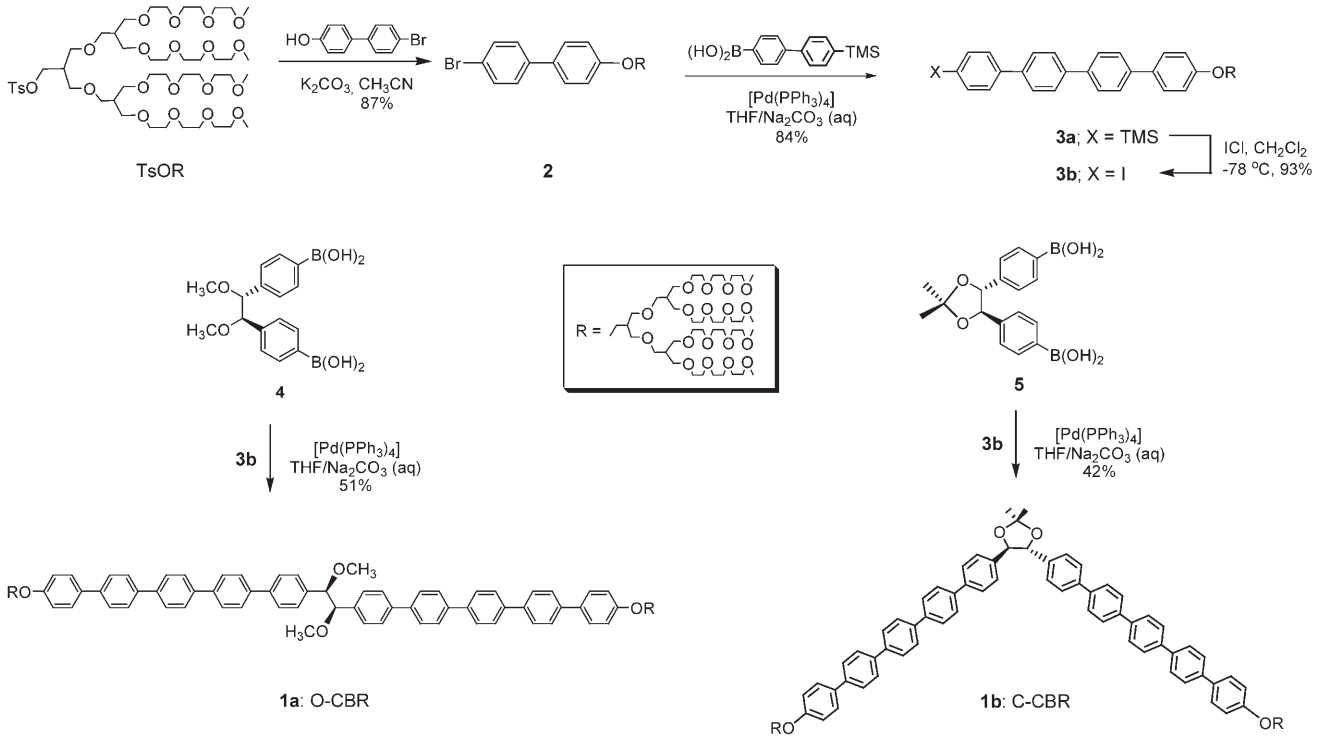

Scheme 1. Synthesis of the CBRs.

based on a closed chiral group, were obtained by Sharpless asymmetric dihydroxylation of *trans*-4,4′-dibromostilbene by using AD-mix β followed by subsequent methylation of the hydroxyl group (**4**) or formation of a ketal from the hydroxyl group (**5**), and finally by replacing the bromide atoms by boronic acid using butyl lithium and triisopropylborate.[18] The basic synthetic methodology to generate such a flexible dendrimer employed a facile convergent route, as reported previously.[19] The first step was performed by the etherification of 4,4′-bromohydroxy biphenyl with the tosylated dendron under basic conditions. The elongated rod building block, **3a**, was obtained by a Suzuki coupling reaction of **2** with 4-trimethylsilylbiphenyl-4′-boronic acid. For the next Suzuki coupling reaction, the trimethylsilyl group of **3a** was substituted with aryl iodide, which is the most active reagent in Suzuki type aromatic couplings. The final CBRs were synthesized by following the same sequence of reactions, that is, by the Suzuki coupling reaction of **3b** with chiral boronic acids **4** or **5**.

The resulting CBRs (**1a** (O-CBR) and **1b** (C-CBR)) were characterized by ^{1}H and ^{13}C NMR spectroscopies, polarimetry, and MALDI-TOF mass spectrometry. All of the analytical data were in full agreement with the structures presented. As confirmed by ^{1}H NMR spectroscopy, the ratio of the aromatic protons of the rod building block to the alkyl protons was consistent with the calculated ratio, and the specific rotation values of both molecules obtained by polarimetry appeared to have positive signs with $[\alpha]_D^{20}$ values of +101.4 and +180.4° for O-CBR and C-CBR, respectively. As shown in Figure 1, the MALDI-TOF mass spectra of the molecules exhibit two signals that can be assigned as the Na and K adducts of the molecular ions. The mass that corresponds to a representative peak in the spectrum is matched with the calculated molecular weight of each molecule.

Conformation of chiral bridging moieties: The opened chiral bridging moiety in O-CBR is conformationally flexible and the diol can be assumed to have two limiting conformations, as illustrated in Figure 2a, and the determination of the most stable conformation in a single molecular state is a delicate procedure. In the aggregated state, however, the rigid aromatic building blocks of the O-CBR molecule might favor packing in a parallel fashion to maximize π-stacking interactions.[20] Therefore, the linear conformation (structure B) would be more favorable in the self-assembled state. Similarly, the closed chiral bridging moiety in C-CBR can also have two conformations (Figure 2b). As previously reported,[21] the most stable conformation of the dioxolane ring is structure A′, in which the two aromatic rings have a *quasi*-gauche relationship when viewed along the C*–C* bond. This stability is because the aromatic groups are located closely to the 2,2-methyl groups of the dioxolane ring, which gives rise to steric hindrance in structure B′. Consequently, O-CBR adopts a linear-shape, whereas C-CBR adopts a bent-shape.

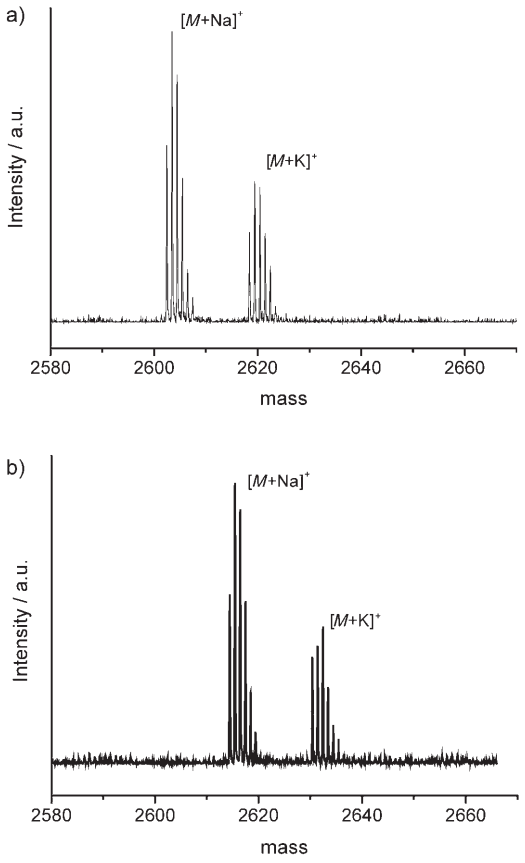

Figure 1. MALDI-TOF mass spectra of a) **1a** (O-CBR) and b) **1b** (C-CBR).

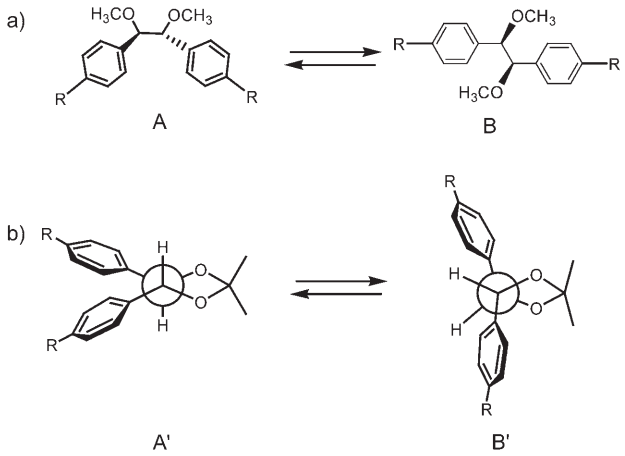

Figure 2. Possible conformations of chiral bridged moieties in CBRs.

Bulk-state structure: The self-assembling behavior of CBRs in the bulk state was investigated by means of DSC, thermal polarized optical microscopy, TEM, and X-ray scattering methods. Figure 3a presents the DSC heating traces of the CBRs. Both molecules showed an ordered bulk-state structure. O-CBR, which is based on the extended rod, showed a liquid crystalline–isotropic transition at 115.2 °C on the heating scan. C-CBR, which is based on the bent-shaped aromat-

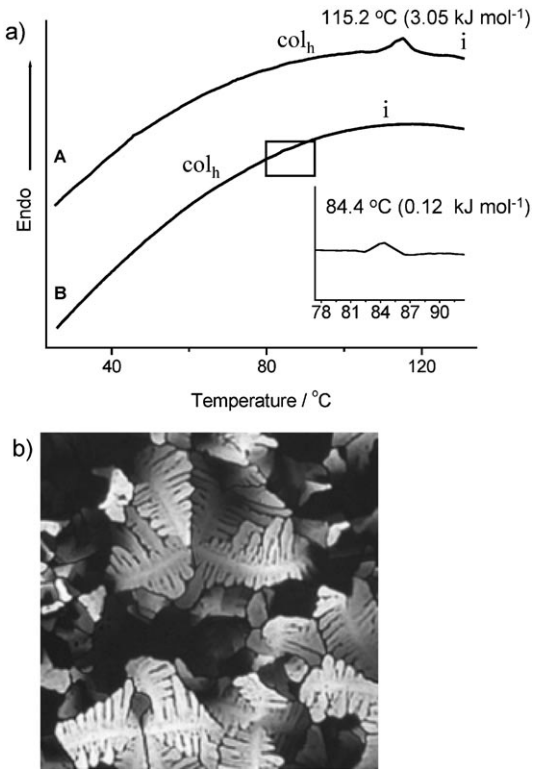

Figure 3. a) DSC traces ($10\,°C\,min^{-1}$) recorded during the first heating scan of A) O-CBR and B) C-CBR. The inset is a magnification of the box indicated on the graph. b) Representative optical polarized micrograph ($100\times$) of the texture exhibited by O-CBR at the transition from the isotropic state at 100 °C.

ic unit, however, showed a significant depression of this transition (84.4 °C). This depression is attributed to the difficulty in packing caused by bent-shaped rigid segments in the liquid-crystalline state. From DSC data, the enthalpy change associated with the liquid crystalline–isotropic transition can be related to the relative degree of liquid-crystalline packing. The heat of fusion ($3.05\,kJ\,mol^{-1}$) of O-CBR was much larger than that of C-CBR ($0.12\,kJ\,mol^{-1}$), which means that the liquid-crystalline ordering of O-CBR is much larger than that of C-CBR. Between cross polarizers, these waxy solids showed strong birefringence. Although no discernible texture could be identified from C-CBR, O-CBR showed a characteristic texture associated with supramolecular ordering. On slow cooling from the isotropic liquid, the formation of unique domains that correspond to a hexagonal columnar texture could be easily observed under a polarized optical microscope (Figure 3b).

To corroborate the bulk-state structure of CBRs, small- and wide-angle X-ray scattering experiments were performed. The small-angle X-ray diffraction (SAXS) pattern of O-CBR displayed three sharp reflections with the ratio of $1:\sqrt{3}:2$ in the low-angle region that can be assigned as a 2D hexagonal columnar structure with a lattice constant of 6.6 nm (Figure 4a). Only a diffuse halo could be observed in the wide-angle X-ray diffraction (WAXS) pattern, which is indicative of liquid-crystalline order with a mean intermolecular distance of 4.5 Å. For further analysis, the sample was cryomicrotomed to a thickness of approximately 50 to 70 nm and stained with RuO_4 vapor and observed by TEM. Figure 4c shows a hexagonal array of dark spots in a matrix of light oligoether segments. The interdomain distance appeared to be approximately 6.6 nm from the TEM images. Considering the lattice constant and extended molecular length (8.7 nm by Corey–Pauling–Koltun (CPK) molecular model), this dimension implies that the rodlike rigid segments arrange axially with their preferred direction within a cross-sectional slice of the column, in which flexible dendrons are located in the periphery of the slice. Calculated from the density ($\approx 1.17\,g\,cm^{-3}$) and the lattice volume, it was estimated that approximately five molecules were necessary to fill a slice of each column that was 4.5 Å thick.[22]

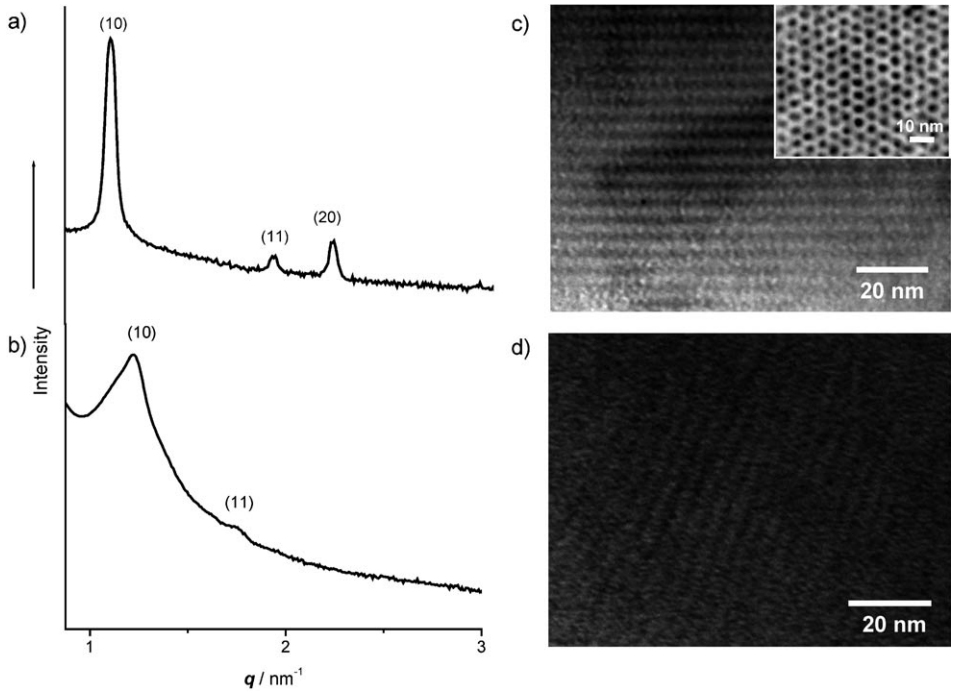

Figure 4. SAXS patterns of a) O-CBR and b) C-CBR at 25 °C, and TEM images of c) O-CBR and d) C-CBR. TEM images of ultramicrotomed films of CBR stained with RuO_4 revealing columnar array of alternating light-colored dendritic layer and dark aromatic layers. The inset image of c) at perpendicular beam incidence shows a hexagonally ordered array of aromatic core of O-CBR.

The SAXS pattern of C-CBR also showed two reflections in the ratio of 1:$\sqrt{3}$ in the low-angle region (Figure 4b). This means that C-CBR also self-assembles into a 2D hexagonal columnar structure with a lattice constant of 6.0 nm. As shown in Figure 4d, the TEM image of C-CBR shows the columnar array. Calculated from the experimental values of the intercolumnar distance (6.0 nm) and the density ($\approx$1.15 g cm^{-3}), the average number of C-CBR molecules in a single slice of the cylinders with a thickness of 4.5 Å (as discussed above) was found to be approximately four.

CD in the bulk state: One can easily imagine that the columns within the mesophase adopt a helical organization because both CBRs are enantiomerically pure. CD experiments were subsequently carried out for the purpose of studying the optical activity in the liquid-crystalline states. The sample was prepared by sandwiching the material between two quartz plates. In this system, the values of linear dichroism (LD), which can be related to the CD values in an oriented system, are negligibly smaller than those arising from CD.[23] The CD spectra did not change appreciably when the sample was rotated in the plane perpendicular to the light beam to eliminate any effects of linear birefringence and linear dichroism by averaging CD spectra (measured at the same positions as samples rotated through successive 30° increments).[24] Remarkably, the CD signals of the mesophase in both molecules (O-CBR and C-CBR) showed the opposite sign (Figure 5), although the same molecular chirality (*R*,*R*). O-CBR gives a positive exciton CD spectrum that consists of the positive Cotton effect at high wavelengths and the negative Cotton effect at low wavelengths with the CD signal passing through zero near the absorption maximum of the chromophore. This positive coupling suggests the presence of a right-handed helical arrangement of the transition dipoles of O-CBR molecules.[25] On the other hand, C-CBR showed a negative exciton CD spectrum that consists of the negative first Cotton effect and the positive second Cotton effect, which is indicative of a left-handed helical arrangement.

On the basis of the results described above, the schematic representation can be constructed as shown in Figure 6. In the case of O-CBR, the inner core of the cylinder is composed of a discrete aromatic core with a rectangular cross section, whereas the outer flexible dendrons splay to fill the intercylinder matrix in a similar way to well-known rod–coil molecules previously reported.[20b] When the individual slices stack along the cylinder axis, the rectangular slice stacks on top of each other with mutual rotation in the same direction to avoid the steric hindrance between the bulky dendron units, which leads to a one-handed helical column. This formation process is similar to that of other helical structures of self-assembling molecules that are based on a conjugated rod block.[15] The specific handedness of this helical column arises from steric constraints imposed by the chiral centers in the rigid segment. As described above, the aromatic segment adopts the linear rod-shaped conformation to maximize π–π interactions between aromatic segments in aggregated states. To pack efficiently, the methoxy group in the chiral segments moves toward the inside, and subsequently, bis(penta-*p*-phenylene) groups twist to reduce steric hindrance between the phenyl and methoxy groups, which results in the propellerlike conformation of the bis(penta-*p*-phenylene) groups (Figure 6b). As a result, this propellerlike structure stacks into a right-handed (*P*) supramolecular helical column.

In contrast, the C-CBR molecule based on a bent-shaped aromatic segment is able to form the columnar slice that is

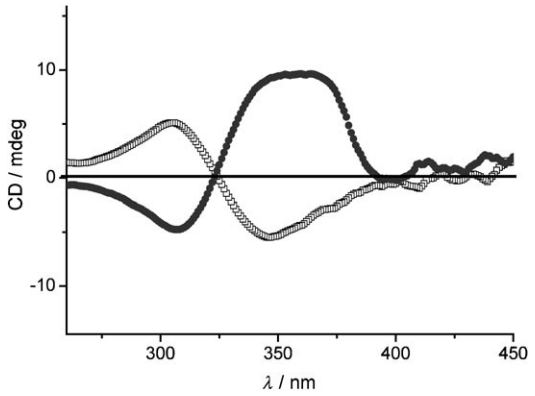

Figure 5. Averaging CD spectra of thin films of CBRs. □: C-CBR and ●: O-CBR.

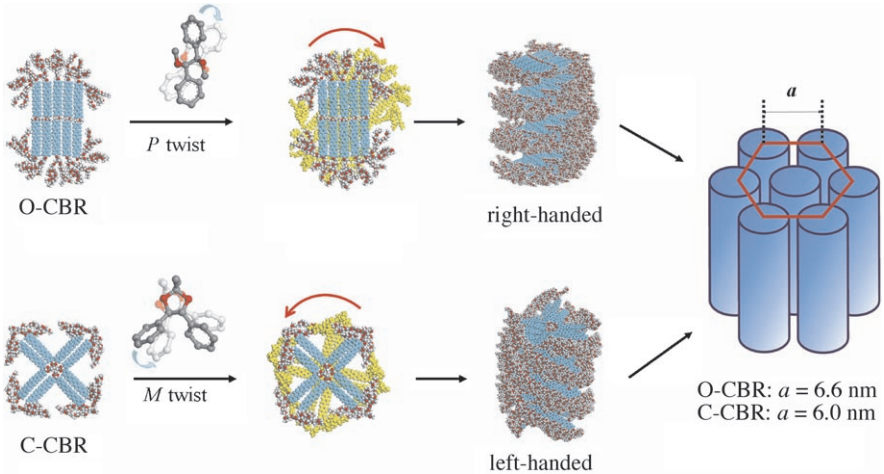

Figure 6. Schematic representation of the hexagonal columnar structure of O-CBR and C-CBR in the bulk state. The opened chiral bridging group packs in a right-handed (*P*) manner and the closed chiral bridging group packs in a left-handed (*M*) manner.

arranged in a coplanar geometry, in which four molecules comprise a single stratum of the cylinder (Figure 6). This packing structure is similar to that formed from polycatenar bent-shaped molecules.[26] It was proposed that a few molecules self-assemble to form an overall disk-shaped object similar to discotic dendrimers.[27] Figure 6 also shows a plausible way in which the closed chiral bridging moieties stack. This group adopts a *quasi*-bisected conformation with the plane of the phenyl group rotated towards the C*–O bond of the oxalane ring. In this type of conformation, the bis(-penta-*p*-phenylene) groups in C-CBR are distorted to result in the left-handed (*M*) supramolecular helix.[21] These results demonstrate that the helical handedness can be manipulated by tailoring the chiral bridging moiety in CBRs.

Aggregation behavior in aqueous solution: CBRs, when dissolved in a selective solvent for one of the blocks, can self-assemble into an aggregate structure because of its amphiphilic characteristics. The aggregation behavior of the molecules was subsequently studied in aqueous solution by using UV-visible and fluorescence spectroscopies. The absorption spectrum of the CBR molecule in aqueous solution (0.005 wt %) exhibits a broad transition with a maximum at $\lambda = 329$ and 325 nm for O-CBR and C-CBR, respectively, which results from the conjugated rod block (Figure 7). The fluorescence spectrum of a solution of the CBR molecule in chloroform (0.005 wt %) exhibits a strong emission maximum at $\lambda = 400$ and 410 nm for O-CBR and C-CBR, respectively. However, the emission maximum in aqueous solution is redshifted with respect to that observed in chloroform, and the fluorescence is significantly quenched, which is indicative of aggregation of the conjugated rod segments.[15] DLS experiments were performed with CBRs in aqueous solution to further investigate the aggregation behavior. The CONTIN analysis of the autocorrelation function of CBR showed a broad peak that corresponds to a hydrodynamic radius (R_H) that ranges from several nanometers to hundreds of nanometers (Figure 7c). The formation of cylindrical micelles was confirmed by the Kratky plot that shows a linear angular dependence over the scattering light intensity of the aggregates (Figure 7d).[28]

The dilute aqueous solutions of CBR displayed a significant Cotton effect in the chromophore of the aromatic unit (Figure 8), which indicates the presence of elongated helical fibrillar aggregates in solution. This is in sharp contrast to the molecularly dissolved state (a solution in chloroform), which does not form a micellar structure and has a very weak Cotton effect. The CD signals of both molecules in solution in chloroform showed the same signals, which is indicative of the same molecular chirality. However, the significant Cotton effect observed in aqueous solution is considered to be the result of the presence of elongated cylindrical

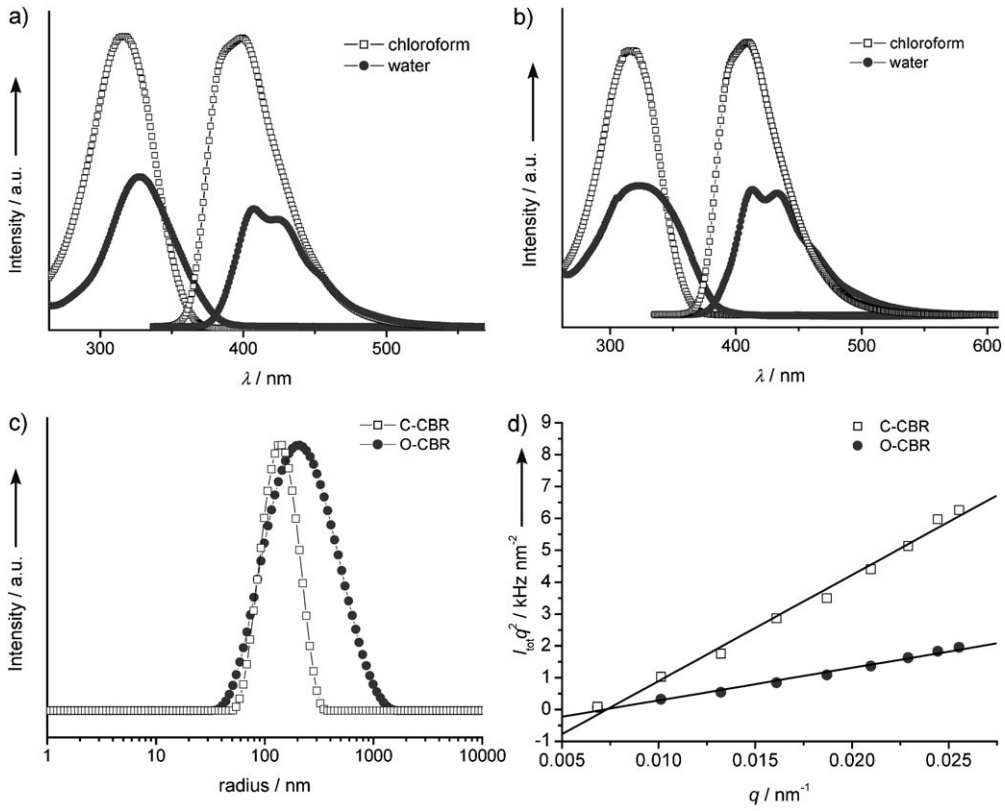

Figure 7. Absorption (left) and emission (right) spectra of the aqueous solution (0.005 wt %, solid line) and solution in chloroform (dashed line) of a) O-CBR and b) C-CBR. c) The size distribution graph obtained by DLS at scattering angle of 90° (from CONTIN analysis of the autocorrelation function). d) Kratky plot and linear fit confirmed the formation of a cylindrical micelle in aqueous solution ($c = 0.05\ g\,L^{-1}$).

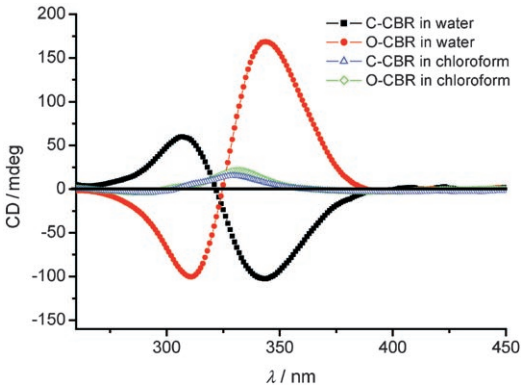

Figure 8. CD spectra of CBRs in aqueous solution and in chloroform (20 μM).

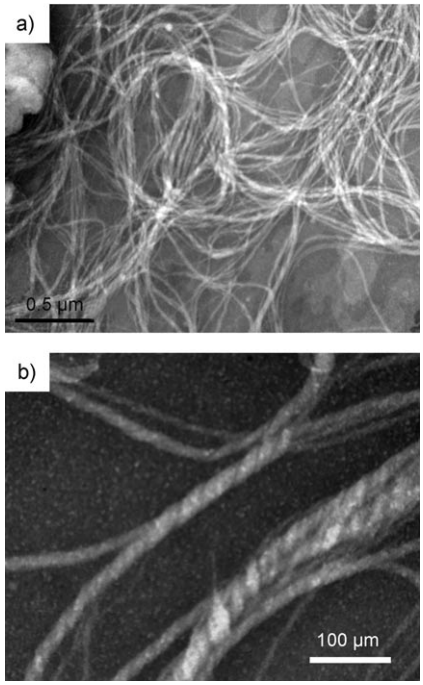

Figure 9. a) TEM image of O-CBR with negative staining (0.005 wt%), and b) magnification in THF/water (1:10).

aggregates with a chiral supramolecular structure of O-CBR or C-CBR, which is similar to the bulk states. This result indicates that the molecular chirality is transferred to the aromatic segments and is subsequently amplified through the formation of a supramolecular helix. As shown in Figure 8, the CD signals of both molecules in aqueous solution are identical to those in the bulk states. It should be noted that both molecules, which have the same chirality (*R*,*R*), showed opposite CD signals. This strongly suggests that the cylindrical structures in aqueous solution are self-assembled in an identical way to the bulk-state π–π stacking of the aromatic segments, as proposed in Figure 6.

The evidence for the formation of the helical aggregates was also provided by TEM experiments (Figure 9). The micrographs of O-CBR that were negatively stained with an aqueous solution of uranyl acetate (2 wt%) showed left-handed twisted bundles of cylindrical aggregates, which were nanometers in diameter and micrometers in length. As discussed earlier, the CD signal demonstrated that the molecules within an elementary fiber are organized into a right-handed helix. Therefore, it can be concluded that the elementary fibers further self-assemble, in a hierarchical fashion, to form a supercoiled structure with opposite helicity. It has been reported that one-handed helices give rise to a supercoiled structure with an opposite helicity through a stepwise hierarchical assembly process.[6,29]

To further investigate this helical inversion, we synthesized (*S*,*S*)-O-CBR as an enantiomer of O-CBR. As expected, the CD spectrum of (*S*,*S*)-O-CBR showed the opposite signal to O-CBR, which has an exciton-coupled bisignate signal with negative ($\lambda_{max}=344$ nm) and positive ($\lambda_{max}=306$ nm) values, which is indicative of a left-handed helix, and as expected, a racemic mixture of O-CBR does not have a CD signal (Figure 10a). In great contrast to the (*R*,*R*) enantiomer, the left-handed helices further assembled hierarchically to form left-handed twisted bundles, as shown by TEM images (Figure 10b). These results indicate that the elementary fibrils formed initially with a left- or right-handed helix may be further coiled in the same direction to form a superhelical structure that is only left-handed (Figure 11). In the case of

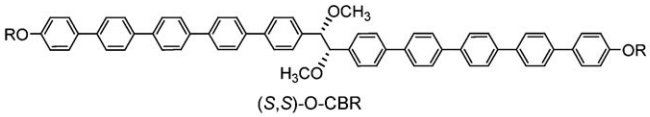

(*S*,*S*)-O-CBR

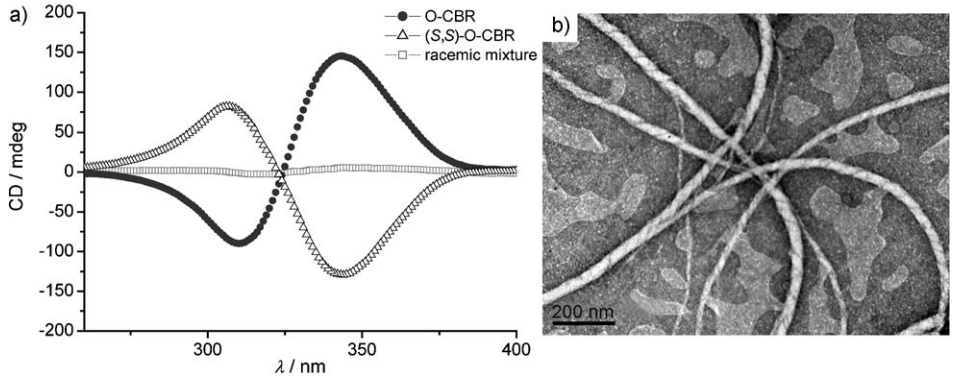

Figure 10. a) CD spectra of O-CBR, (*S*,*S*)-O-CBR, and a racemic mixture in aqueous solution (0.005 wt%). b) TEM image of (*S*,*S*)-O-CBR with negative staining (0.005 wt%) in THF/water (1:10).

C-CBR, although the aggregated helical structure could not be identified, most probably owing to the loss of ordering during the drying process, C-CBR also self-assembled into helical objects in aqueous solution, similar to the bulk state, as given by the results from DLS and CD experiments.

The racemic mixtures are known not to have a Cotton effect,[13,14] which is consistent with our results shown in Figure 10a. In sharp contrast, when O-CBR (20 μM) was added to a solution of C-CBR (20 μM), an unpredictable amplification of the CD intensity was observed (Figure 12a). To investigate this phenomenon in more detail, we carried out CD experiments of the aqueous solutions with the various proportions of O-CBR and C-CBR at a constant total concentration (0.005 wt%). As the O-CBR ratio increases to 50 mol% relative to C-CBR, the resulting CD spectra showed no change in either the shape or the intensity (Figure 12b). Above this molar ratio (C-CBR/(C-CBR+O-CBR) = 50%), the CD intensity at 343 nm, which is the most intensive peak, gradually increases and finally the inversion of the CD signal was observed. More importantly, no change in the CD signal up to an O-CBR concentration of 50 mol% relative to C-CBR indicates that O-CBR adopts a left-handed helical conformation triggered by co-assembly with C-CBR. These results imply that by increasing the molar ratio, O-CBR co-assembles with C-CBR up to a certain ratio, above which the excess O-CBR might be separated and self-assemble into helical fibers with their original handedness.

This phenomenon can be rationalized by considering the conformational flexibility induced by bond rotation in the chiral bridging moiety. The conformation of the chiral bridging group of C-CBR has a bent shape in structure A′, as shown in Figure 2b. This conformation prevents the free rotation of the chiral C*–C* bond by ring closure, whereas O-CBR is able to freely rotate. Therefore, O-CBR can co-assemble with C-CBR through a bent-shaped conformation into left-handed helical fibers, which means that C-CBR acts as a chiral template for the conformational change of O-CBR.

Conclusion

CBRs were synthesized and their self-assembling behavior in both the bulk and solution states was investigated. In the bulk state, the CBRs based on an O-CBR was observed to self-assemble into a right-handed columnar structure, whereas the molecule based on a C-CBR self-assembles into a left-handed columnar structure. In aqueous solution, both amphiphiles self-assemble into well-defined nanofibers with opposite handedness, as confirmed by CD measurements. Two enantiomers of O-CBR self-assemble into helical fibers with opposite handedness. Remarkably, both left- and right-handed helices were shown to further assemble in a hierarchical manner to form only a left-handed superhelical structure. In addition, when O-CBR was added to a solution of C-CBR, the CD signal was amplified. This implies that both molecules co-assemble into a one-handed helix because conformationally flexible O-CBR is able to adopt a bent-shaped conformation for homochiral interactions with C-CBR. These results demonstrate that the handedness of helical fibers can be manipulated by small structural variations in the chiral bridging unit of the chiral rod, both in the bulk and solution states.

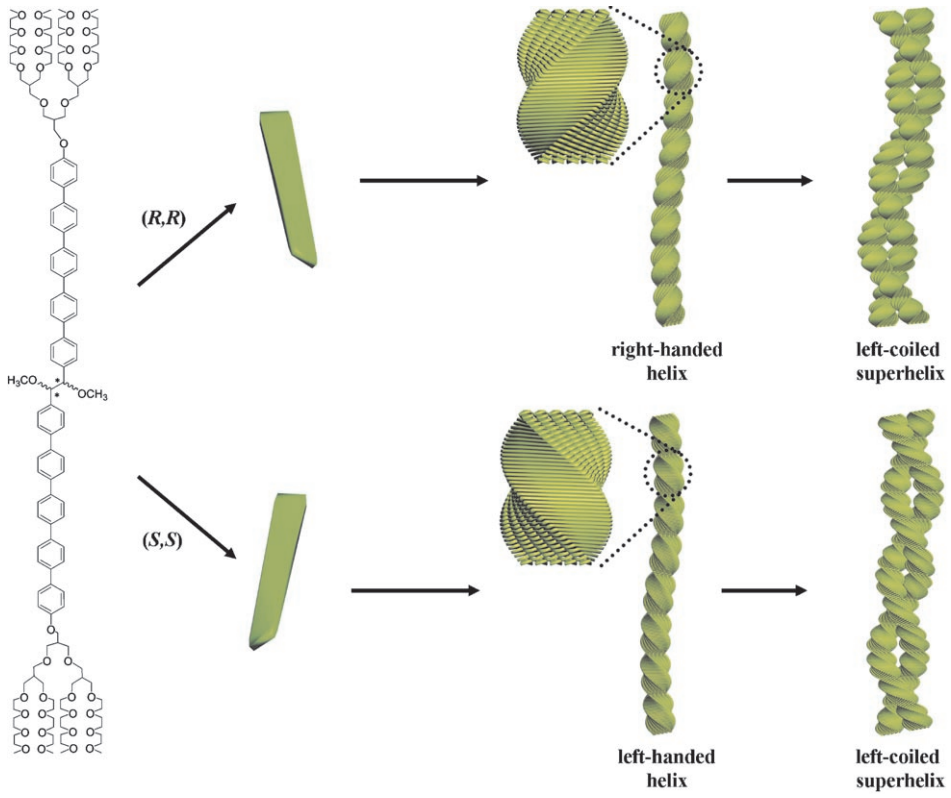

Figure 11. Schematic representation of one-handed helices and hierarchically assembled superhelices with the left-handedness of O-CBR enantiomers.

Experimental Section

Materials: 4-Bromo-4′-hydroxybiphenyl (99%), tetrakis(triphenylphosphane)palladium(0) (99%), and toluene-*p*-sulfonyl chloride (98%) from Tokyo Kasei were used as received. Triethylene glycol and chlorotrimethylsilane (98%) from Aldrich and the other conventional reagents were also used as received. Hexane, dichloromethane, and ethyl acetate were distilled before use. Dry THF was obtained by vacuum transfer from sodium and ben-

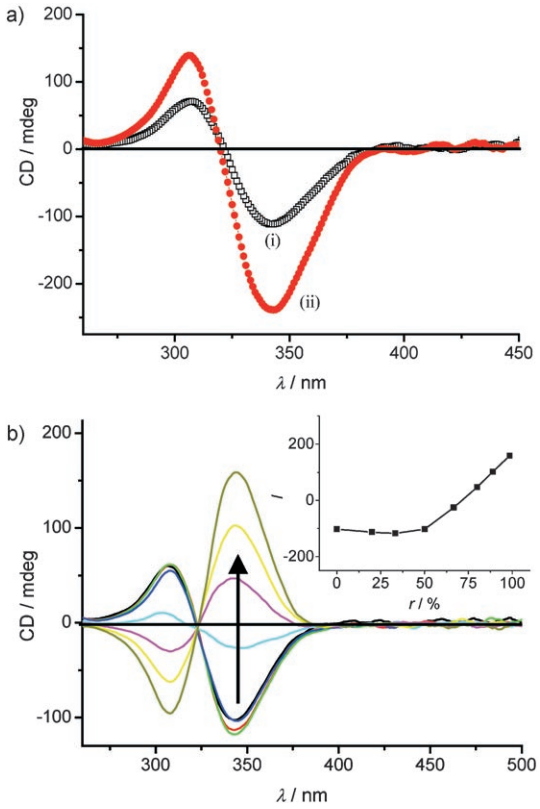

Figure 12. a) CD spectra of CBRs: i) C-CBR (20 μM); ii) CBR mixture solution of C-CBR (20 μM) and O-CBR (20 μM). b) CD spectra CBRs as the C-CBR ratio increases at a constant total concentration of 0.005 wt% in aqueous solution. The inset shows the CD intensity at 343 nm (I) as a function of the molar ratio (r) of O-CBR/(O-CBR+C-CBR).

zophenone. Visualization of TLC plates was accomplished with UV light or iodine vapor. Compounds were synthesized according to the procedure described in Scheme 1. 4,4′-(Trimethylsilyl)biphenylboronic acid and dendritic oligoether (TsOR) were prepared according to the same procedures described previously. Compounds **4** and **5** were prepared according to literature procedures.

Techniques: ^{1}H NMR and ^{13}H NMR spectra were recorded as solutions in $CDCl_3$ by using a Bruker AM 250 spectrometer. The purity of the products was determined by TLC (Merck, silica gel 60). A Perkin–Elmer Diamond DSC differential scanning calorimeter was used to determine the thermal transitions, which were reported as the maxima and minima of their endothermic or exothermic peaks. In all cases, the heating and cooling rates were 10 °C min^{-1}. X-ray scattering measurements were performed in transmission mode with synchrotron radiation at the 10C1 X-ray beam line at the Pohang Accelerator Laboratory, Korea. MALDI-TOF MS was performed by using a Perseptive Biosystems Voyager-DE STR instrument with a 2,5-dihydroxy benzoic acid matrix. DLS measurements were performed by using an ALV/CGS-3 Compact Goniometer System instrument. UV/Vis absorption spectra were obtained by using a Shimadzu 1601 UV spectrometer. The fluorescence spectra were obtained by using a Hitachi F-4500 fluorescence spectrometer. CD spectra were obtained by using a JASCO J-810 spectropolarimeter. TEM was performed at 120 kV by using a JEOL-JEM 2010 microscope.

TEM measurements: A drop of a solution of O-CBR (0.005 wt%) in THF/water (1:10) was placed onto a carbon-coated copper grid and dried at room temperature before it was subsequently negatively stained with an aqueous solution of uranyl acetate (2 wt%).

Synthesis: The synthetic procedures used in the preparation of the CBRs are described in Scheme 1.

Synthesis of ***2***: 4′-Bromo-biphenyl-4-ol (2.15 g, 8.64 mmol), TsOR (2.21 g, 2.16 mmol), and excess K_2CO_3 were dissolved in anhydrous acetonitrile (100 mL). The mixture was heated at reflux overnight and then cooled to room temperature. The solvent was removed by using a rotary evaporator and the resulting mixture was poured into water (50 mL) and extracted with CH_2Cl_2. The aqueous layer was washed with water, dried over anhydrous $MgSO_4$, and filtered. Purification of the residue by flash column chromatography on silica gel by using CH_2Cl_2 and ethyl acetate/methanol (8:1 v/v) as the eluent to yield **2** as a colorless liquid (2.00 g, 88.6%). ^{1}H NMR (250 MHz, $CDCl_3$): δ = 7.54–7.33 (m, 6H; Ar-H), 6.96 (d, J = 8.7 Hz, 2H; Ar-H, *m* to OCH_2), 4.03 (d, J = 5.7 Hz, 2H; CH_2Ophenyl), 3.63–3.45 (m, 64H; OCH_2), 3.38–3.34 (m, 12H; OCH_3), 2.39–2.35 (m, 1H; phenylO$CH_2CH(CH_2O)_2$), 2.17–2.06 ppm (m, 2H; $CH(CH_2O)_2$).

Synthesis of ***3a*** *and* ***3b***: Compound **3** (2.00 g, 1.82 mmol) and 4,4′-(trimethylsilyl)biphenylboronic acid (0.846 g, 2.73 mmol) were dissolved in degassed THF (40 mL). Degassed 2 M aqueous Na_2CO_3 (20 mL) was added to the solution before tetrakis(triphenylphosphine)palladium(0) (10 mg, 0.009 mmol) was added. The mixture was heated at reflux for 48 h with vigorous stirring under nitrogen. The solution was then cooled to room temperature, the layers were separated, and the aqueous layer was then washed with CH_2Cl_2 (2×). The combined organic layers were dried over anhydrous $MgSO_4$ and filtered. The solvent was removed by using a rotary evaporator and the crude product was purified by column chromatography (silica gel) by using ethyl acetate/methanol (8:1 v/v) as the eluent to yield **3a** as a colorless liquid (1.91 g, 84.3%). Subsequently, compound **3a** (0.776 g, 0.625 mmol) was dissolved in CH_2Cl_2 (300 mL) at −78 °C and a 1.0 M solution of ICl in CH_2Cl_2 (1.87 mL, 1.87 mmol) was added dropwise. The reaction mixture was stirred for 1 h under nitrogen before 1 M aqueous $Na_2S_2O_5$ (15 mL) solution was added and the solution was stirred for 4 h. The layers were separated, and the aqueous layer was then washed with CH_2Cl_2 (2×). The combined organic layers were dried over anhydrous $MgSO_4$ and filtered. The solvent was removed by using a rotary evaporator and the crude product was purified by column chromatography (silica gel) by using CH_2Cl_2/methanol (8:1 v/v) as the eluent to yield **3b** as a colorless liquid (0.750 g, 92.6%).

3a: ^{1}H NMR (250 MHz, $CDCl_3$): δ = 7.70–7.55 (m, 14H; Ar-H), 6.99 (d, J = 8.4 Hz, 2H; Ar-H, *o* to OCH_2), 4.05 (d, J = 5.5 Hz, 2H; CH_2Ophenyl), 3.51–3.76 (m, 64H; OCH_2), 3.29–3.27 (m, 12H; OCH_3), 2.39–2.35 (m, 1H; phenylO$CH_2CH(CH_2O)_2$), 2.17–2.06 (m, 2H; $CH(CH_2O)_2$), 0.31 ppm (s, 9H; phenylSi$(CH_3)_3$).

3b: ^{1}H NMR (250 MHz, $CDCl_3$): δ = 7.77 (d, J = 8.3 Hz, 2H; Ar-H, *o* to I), 7.72–7.54 (m, 10H; Ar-H), 7.37 (d, J = 8.4 Hz, 2H; Ar-H, *m* to I), 6.99 (d, J = 8.4 Hz, 2H; Ar-H, *o* to OCH_2), 4.05 (d, J = 5.5 Hz, 2H; CH_2Ophenyl), 3.51–3.76 (m, 64H; OCH_2), 3.29–3.27 (m, 12H; OCH_3), 2.39–2.35 (m, 1H; phenylO$CH_2CH(CH_2O)_2$), 2.17–2.06 ppm (m, 2H; $CH(CH_2O)_2$).

Synthesis of ***4***: A solution of *n*-butyllithium (9.5 mL of 1.6 M solution in hexane, 15.1 mmol) was added slowly to a solution of (*1R*,*2R*)-1,2-bis(4-bromophenyl)-1,2-dimethoxyethane (1.5 g, 3.78 mmol) in dry THF (50 mL) at −78 °C under a nitrogen atmosphere. After stirring for 30 min at −78 °C, triisopropyl borate (6.9 mL, 30 mmol) was added, and the reaction mixture was stirred for 12 h. The reaction was quenched with a 1 M aqueous solution of HCl (50 mL) and extracted with ethyl acetate. The crude organic extract was treated with a 1 M aqueous solution of NaOH (3×100 mL). The combined aqueous extracts were acidified with concd HCl and extracted with ethyl acetate. The organic extracts were combined, washed with brine, dried over anhydrous $MgSO_4$, and filtered. Solvent was removed by using a rotary evaporator and the crude product was purified by column chromatography (silica gel) by using CH_2Cl_2/methanol (10:1 v/v) as the eluent to yield **4** as a white solid (0.68 g, 54.9%). ^{1}H NMR (250 MHz, CD_3OD): δ = 7.40 (d, J = 7.6 Hz, 4H; *o* to $B(OH)_2$), 7.00 (d, J = 7.6 Hz, 4H; *m* to $B(OH)_2$), 4.33 (s, 2H; (CH_3O)(phenyl)CH), 3.30 ppm (s, 6H; CHOCH_3).

Synthesis of compound ***5***: A solution of *n*-butyllithium (5.0 mL of 1.6 M solution in hexane, 8.0 mmol) was added slowly to a solution of (*4R*,*5R*)-4,5-bis(4-bromophenyl)-2,2-dimethyl-1,3-dioxolane (0.82 g, 1.99 mmol) in dry THF (50 mL) at −78 °C under a nitrogen atmosphere. After stirring

for 30 min at −78 °C, triisopropyl borate (5 mL, 20 mmol) was added and the reaction mixture was stirred for 12 h. The reaction was quenched with a 1 M aqueous solution of HCl (50 mL) and extracted with ethyl acetate. The crude organic extract was treated with a 1 M aqueous solution of NaOH (3×100 mL). The combined aqueous extracts were acidified with concd HCl and extracted with ethyl acetate. The organic extracts were combined, washed with brine, dried on anhydrous $MgSO_4$, and filtered. The solvent was removed by using a rotary evaporator and the crude product was purified by column chromatography (silica gel) by using CH_2Cl_2/methanol (10:1 v/v) as the eluent to yield **5** as a white solid (0.31 g, 45.1 %). ^{1}H NMR (250 MHz, DMSO): δ = 8.06 (s, 4H; phenyl-B*(OH)$_2$*), 7.75 (d, J = 7.6 Hz, 4H; *o* to B(OH)$_2$), 7.18 (d, J = 7.6 Hz, 4H; *m* to B(OH)$_2$), 4.74 (s, 2H; ((CH$_3$)$_2$CO)(phenyl)*CH*), 1.59 ppm (s, 6H; CHOC*(CH$_3$)$_2$*).

Synthesis of ***1a*** *(O-CBR) and* ***1b*** *(C-CBR)*: These compounds were synthesized by using the same procedure. A representative example is described for **1a**. Compound **3b** (0.300 g, 0.231 mmol) and **4** (0.038 g, 0.077 mmol) were dissolved in degassed THF (20 mL). Degassed 2 M aqueous Na_2CO_3 (10 mL) was added to the solution before tetrakis(triphenylphosphine)palladium(0) (10 mg, 0.009 mmol) was added. The mixture was heated at reflux for 48 h with vigorous stirring under nitrogen. The solution was cooled to room temperature, the layers were separated, and the aqueous layer was then washed with CH_2Cl_2 (2×). The combined organic layers were dried over anhydrous $MgSO_4$ and filtered. The solvent was removed by using a rotary evaporator and the crude product was purified by column chromatography (silica gel) by using CH_2Cl_2/methanol (8:1 v/v) as the eluent to yield **1a** as a white waxy solid (100 mg, 50.5 %).

1a (O-CBR): Yield = 50.5 %; $[\alpha]_D^{20}$ = + 101.4° (c = 0.00053 g mL^{-1}, $CHCl_3$); ^{1}H NMR (250 MHz, $CDCl_3$): δ = 7.73–7.50 (m, 32H; Ar-H), 7.16 (d, J = 8.1 Hz, 2H; Ar-H, *m* to CHOCH$_3$), 7.00 (d, J = 8.6 Hz, 2H; Ar-H, *o* to OCH$_2$), 4.43 (s, 2H; Ar*CH*OCH$_3$), 4.06 (d, J = 5.2 Hz, 4H; *CH*$_2$Ophenyl), 3.64–3.46 (m, 128H; O*CH*$_2$), 3.39–3.36 (m, 24H; O*CH*$_3$), 2.39–2.35 (m, 2H; phenylOCH$_2$*CH*(CH$_2$O)$_2$), 2.20-2.17 ppm (m, 4H; *CH*-(CH$_2$O)$_2$); ^{13}C NMR (63 MHz, $CDCl_3$): δ = 158.9, 140.0, 139.8, 139.7, 139.6, 138.9, 137.5, 133.1, 128.6, 128.1, 127.5, 127.4, 127.2, 126.5, 115.0, 88.1, 72.0, 70.7, 70.6, 70.5, 69.8, 69.6, 59.1, 57.4, 40.2, 40.1 ppm; MALDI-TOF MS: m/z: 2602.48 [M+Na]$^+$, 2618.41 [M+K]$^+$.

1b (C-CBR): Yield = 42.1 %; $[\alpha]_D^{20}$ = + 180.4° (c = 0.00058 g mL^{-1}, $CHCl_3$); ^{1}H NMR (250 MHz, $CDCl_3$) δ = 7.74–7.63 (m, 32H; Ar-H), 7.38 (d, J = 8.3 Hz, 2H; Ar-H, *m* to CHOC(CH$_3$)$_2$), 7.00 (d, J = 8.6 Hz, 2H; Ar-H, *o* to OCH$_2$), 4.88 (s, 2H; Ar*CH*OC(CH$_3$)$_2$), 4.06 (d, J = 5.4 Hz, 4H; *CH*$_2$Ophenyl), 3.65–3.47 (m, 128H; O*CH*$_2$), 3.39–3.36 (m, 24H; O*CH*$_3$), 2.39–2.35 (m, 2H; phenylOCH$_2$*CH*(CH$_2$O)$_2$), 2.20–2.17 (m, 4H; *CH*(CH$_2$O)$_2$) 1.74 ppm (s, 6H; ArCHOC*(CH$_3$)$_2$*); ^{13}C NMR (63 MHz, $CDCl_3$) δ = 158.9, 139.9, 139.8, 139.7, 139.6, 138.9, 137.5, 131.1, 128.5, 128.1, 127.6, 127.5, 127.4, 127.2, 126.5, 114.9, 110.2, 85.6, 72.0, 70.7, 70.6, 70.5, 69.8, 69.6, 69.4, 59.2, 40.1, 26.1 ppm; MALDI-TOF MS: m/z: 2614.45 [M+Na]$^+$, 2630.41 [M+K]$^+$.

Synthesis of (S,S)*-O-CBR*: (*S*,*S*)-O-CBR was prepared by the same procedure as O-CBR by means of a Suzuki-type aromatic coupling of **3b** and (*S*,*S*)-1,2-bis(4-dihydroxyboranylphenyl)-1,2-dimethoxyethane (obtained by Sharpless asymmetric dihydroxylation of *trans*-4,4′-dibromostilbene by using AD-mix α). $[\alpha]_D^{20}$ = −102.3° (c = 0.00057 g mL^{-1}, $CHCl_3$); ^{1}H NMR (250 MHz, $CDCl_3$): δ = 7.72–7.49 (m, 32H; Ar-H), 7.15 (d, J = 8.1 Hz, 2H; Ar-H, *m* to CHOCH$_3$), 6.99 (d, J = 8.7 Hz, 2H; Ar-H, *o* to OCH$_2$), 4.42 (s, 2H; Ar*CH*OCH$_3$), 4.05 (d, J = 5.2 Hz, 4H; *CH*$_2$Ophenyl), 3.64–3.46 (m, 128H; O*CH*$_2$), 3.37 (m, 24H; O*CH*$_3$), 2.39–2.35 (m, 2H; phenylOCH$_2$*CH*(CH$_2$O)$_2$), 2.20–2.17 ppm (m, 4H; *CH*(CH$_2$O)$_2$); ^{13}C NMR (63 MHz, $CDCl_3$): δ = 158.9, 140.0, 139.8, 139.7, 139.6, 138.9, 137.5, 133.1, 128.6, 128.1, 127.5, 127.4, 127.2, 126.5, 115.0, 88.1, 72.0, 70.7, 70.6, 70.5, 69.8, 69.6, 59.1, 57.4, 40.2, 40.1 ppm; MALDI-TOF MS: m/z: 2602.48 [M+Na]$^+$, 2618.41 [M+K]$^+$.

Acknowledgements

This work was supported by the Creative Research Initiative Program of the Ministry of Science and Technology, Korea. E.L. thanks the Seoul Science Fellowship Program and we acknowledge a fellowship of the BK21 program from the Ministry of Education and Human Resources Development.

[1] a) J.-M. Lehn, *Proc. Natl. Acad. Sci. USA* **2002**, *99*, 4763–4768; b) S. Förster, T. Plantenberg, *Angew. Chem.* **2002**, *114*, 712–739; *Angew. Chem. Int. Ed.* **2002**, *41*, 688–714; c) F. J. M. Hoeben, P. Jonkheijm, E. W. Meijer, A. P. H. J. Schenning, *Chem. Rev.* **2005**, *105*, 1491–1546; d) J. J. L. M. Cornelissen, A. E. Rowan, R. J. M. Nolte, N. A. J. M. Sommerdijk, *Chem. Rev.* **2001**, *101*, 4039–4070.

[2] a) A. Ajayaghosh, C. Vijayakumar, R. Varghese, S. J. George, *Angew. Chem.* **2006**, *118*, 1159–1162; *Angew. Chem. Int. Ed.* **2006**, *45*, 1141–1144; b) Y. Yamamoto, T. Fukushima, Y. Suna, N. Ishii, A. Saeki, S. Seki, S. Tagawa, M. Taniguchi, T. Kawai, T. Aida, *Science* **2006**, *314*, 1761–1764; c) M. Lee, B.-K. Cho, W.-C. Zin, *Chem. Rev.* **2001**, *101*, 3869–3892.

[3] a) V. Percec, A. E. Dulcey, M. Peterca, P. Adelman, R. Samant, V. S. K. Balagurusamy, P. A. Heiney, *J. Am. Chem. Soc.* **2007**, *129*, 5992–6002; b) J. H. K. K. Hirschberg, L. Brunsveld, A. Ramzi, J. A. J. M. Vekemans, R. P. Sijbesma, E. W. Meijer, *Nature* **2000**, *407*, 167–170; c) R. S. Johnson, T. Yamazaki, A. Kovalenko, H. Fenniri, *J. Am. Chem. Soc.* **2007**, *129*, 5735–5743.

[4] a) F. Vera, R. M. Tejedor, P. Romero, J. Barberá, M. B. Ros, J. L. Serrano, T. Sierra, *Angew. Chem.* **2007**, *119*, 1905–1909; *Angew. Chem. Int. Ed.* **2007**, *46*, 1873–1877; b) T. Kato, T. Matsuoka, N. Masayuki, Y. Kamikawa, K. Kanie, T. Nishimura, E. Yashima, S. Ujiie, *Angew. Chem.* **2004**, *116*, 2003–2006; *Angew. Chem. Int. Ed.* **2004**, *43*, 1969–1972; c) M. Inouye, M. Waki, H. Abe, *J. Am. Chem. Soc.* **2004**, *126*, 2022–2027.

[5] T. Ishi-i, R. Kuwahara, A. Takata, Y. Jeong, K. Sakurai, S. Mataka, *Chem. Eur. J.* **2006**, *12*, 763–776.

[6] A. Ajayaghosh, C. Vijayakumar, R. Varghese, S. J. George, *Angew. Chem.* **2006**, *118*, 470–474; *Angew. Chem. Int. Ed.* **2006**, *45*, 456–460.

[7] W.-Y. Yang, E. Lee, M. Lee, *J. Am. Chem. Soc.* **2006**, *128*, 3484–3485.

[8] a) J. C. Nelson, J. G. Saven, J. S. Moore, P. G. Wolynes, *Science* **1997**, *277*, 1793–1796; b) R. B. Prince, L. Brunsveld, E. W. Meijer, J. S. Moore, *Angew. Chem.* **2000**, *112*, 234–236; *Angew. Chem. Int. Ed.* **2000**, *39*, 228–230.

[9] a) H.-J. Kim, W.-C. Zin, M. Lee, *J. Am. Chem. Soc.* **2004**, *126*, 7009–7014; b) K. Kishikawa, S. Furusawa, T. Yamaki, S. Kohmoto, M. Yamamoto, K. Yamaguchi, *J. Am. Chem. Soc.* **2002**, *124*, 1597–1605.

[10] a) D. J. Hill, M. J. Mio, R. B. Prince, T. S. Hughes, J. S. Moore, *Chem. Rev.* **2001**, *101*, 3893–4011; b) R. Oda, I. Huc, S. J. Candau, *Angew. Chem.* **1998**, *110*, 2835–2838; *Angew. Chem. Int. Ed.* **1998**, *37*, 2689–2691; c) J. Makarević, M. Jokić, Z. Raza, Z. Štefanić, B. Kojić-Prodić, M. Žinić, *Chem. Eur. J.* **2003**, *9*, 5567–5580; d) M. S. Spector, J. V. Selinger, A. Singh, J. M. Rodriguez, R. R. Price, J. M. Schnur, *Langmuir* **1998**, *14*, 3493–3500; e) A. R. Hirst, B. Huang, V. Castelletto, I. W. Hamley, D. K. Smith, *Chem. Eur. J.* **2007**, *13*, 2180–2188.

[11] a) A. Tanatani, M. J. Mio, J. S. Moore, *J. Am. Chem. Soc.* **2001**, *123*, 1792–1793; b) H. Fenniri, B.-L. Deng, A. E. Ribbe, *J. Am. Chem. Soc.* **2002**, *124*, 11064–11072; c) V. V. Borovkov, J. M. Lintuluoto, Y. Inoue, *J. Am. Chem. Soc.* **2001**, *123*, 2979–2989; d) M. M. Green, N. C. Peterson, T. Sato, A. Teramoto, S. Lifson, *Science* **1995**, *268*, 1860–1866; e) M. M. Green, J.-W. Park, T. Sato, A. Teramoto, S. Lifson, R. L. B. Selinger, J. V. Selinger, *Angew. Chem.* **1999**, *111*, 3328–3345; *Angew. Chem. Int. Ed.* **1999**, *38*, 3138–3154; f) K. Tang, M. M. Green, K. S. Cheon, J. V. Selinger, B. A. Garetz, *J. Am. Chem. Soc.* **2003**, *125*, 7313–7323.

[12] a) K. Maeda, H. Mochizuki, M. Watanabe, E. Yashima, *J. Am. Chem. Soc.* **2006**, *128*, 7639–7650; b) D. Pijper, B. L. Feringa,

Angew. Chem. **2007**, *119*, 3767–3770; *Angew. Chem. Int. Ed.* **2007**, *46*, 3693–3696; c) S. Tomar, M. M. Green, L. A. Day, *J. Am. Chem. Soc.* **2007**, *129*, 3367–3375.

[13] Ph. Leclère, M. Surin, P. Viville, R. Lazzaroni, A. F. M. Kilbinger, O. Henze, W. J. Feast, M. Cavallini, F. Biscarini, A. P. H. J. Schenning, E. W. Meijer, *Chem. Mater.* **2004**, *16*, 4452–4466.

[14] B. W. Messmore, P. A. Sukerkar, S. I. Stupp, *J. Am. Chem. Soc.* **2005**, *127*, 7992–7993.

[15] a) A. P. H. J. Schenning, A. F. M. Kilbinger, F. Biscarini, M. Cavallini, H. J. Cooper, P. J. Derrick, W. J. Feast, R. Lazzaroni, Ph. Leclère, L. A. McDonell, E. W. Meijer, S. C. J. Meskers, *J. Am. Chem. Soc.* **2002**, *124*, 1269–1275; b) J. van Herrikhuyzen, A. Syamakumari, A. P. H. J. Schenning, E. W. Meijer, *J. Am. Chem. Soc.* **2004**, *126*, 10021–10027; c) P. Jonkheijm, F. J. M. Hoeben, R. Kleppinger, J. van Herrikhuyzen, A. P. H. J. Schenning, E. W. Meijer, *J. Am. Chem. Soc.* **2003**, *125*, 15941–15949; d) J. van Gestel, A. R. A. Palmans, B. Titulaer, J. A. J. M. Vekemans, E. W. Meijer, *J. Am. Chem. Soc.* **2005**, *127*, 5490–5494; e) O. Henze, J. Feast, F. Gardebien, P. Jonkheijm, R. Lazzaroni, Ph. Leclère, E. W. Meijer, A. P. H. J. Schenning, *J. Am. Chem. Soc.* **2006**, *128*, 5923–5929.

[16] J. Bae, J.-H. Choi, Y.-S. Yoo, N.-K. Oh, B.-S. Kim, M. Lee, *J. Am. Chem. Soc.* **2005**, *127*, 9668–9669.

[17] J.-H. Ryu, H.-J. Kim, Z. Huang, E. Lee, M. Lee, *Angew. Chem.* **2006**, *118*, 5430–5433; *Angew. Chem. Int. Ed.* **2006**, *45*, 5304–5307.

[18] K. S. Jeong, S. Y. Kim, U.-S. Shin, M. Kogej, N. T. M. Hai, P. Broekmann, N. Jeong, B. Kirchner, M. Reiher, C. A. Schalley, *J. Am. Chem. Soc.* **2005**, *127*, 17672–17685.

[19] C.-J. Jang, J.-H. Ryu, J.-D. Lee, D. Sohn, M. Lee, *Chem. Mater.* **2004**, *16*, 4226–4231.

[20] a) J.-H. Ryu, N.-K. Oh, W.-C Zin, M. Lee, *J. Am. Chem. Soc.* **2004**, *126*, 3551–3558; b) M. Lee, B.-K. Cho, H. Kim, J.-Y. Lee, W.-C. Zin, *J. Am. Chem. Soc.* **1998**, *120*, 9168–9179.

[21] a) C. Rosini, G. P. Spada, G. Proni, S. Masiero, S. Scamuzzi, *J. Am. Chem. Soc.* **1997**, *119*, 506–512; b) S. Superchi, M. I. Donnoli, G. Proni, G. P. Spada, C. Rosini, *J. Org. Chem.* **1999**, *64*, 4762–4767; c) C. Rosini, S. Scamuzzi, G. Uccello-Barretta, P. Salvadori, *J. Org. Chem.* **1994**, *59*, 7395–7400; d) G. Gottarelli, P. Mariani, G. P. Spada, B. Samorì, A. Forni, G. Solladié, H. Hibert, *Tetrahedron* **1983**, *39*, 1337–1344.

[22] From the experimental values of the intercolumnar distance (a) and the densities (ρ), the average number (n) of molecules arranged side by side in a single slice of the cylinders with a thickness (h) of 4.5 Å can be calculated by using to following equation, in which M is the molecular mass and N_A is Avogadro's number: $n=\frac{\sqrt{3}}{2}a^2 h\frac{N_A}{M}\rho$.

[23] a) K. Murata, M. Aoki, T. Suzuki, T. Harada, H. Kawabata, T. Komri, F. Ohseto, K. Ueda, S. Shinkai, *J. Am. Chem. Soc.* **1994**, *116*, 6664–6676; b) See the Supporting Information.

[24] C. Nuckolls, T. J. Katz, T. Verbiest, S. V. Elshocht, H.-G. Kuball, S. Kiesewalter, A. J. Lovinger, A. Persoons, *J. Am. Chem. Soc.* **1998**, *120*, 8656–8660.

[25] N. Berova, K. Nakanishi in *Circular Dichroism: Principle and Application*, 2nd ed. (Eds.: N. Berova, K. Nakanishi, R. W. Woody), Wiley-VCH, Weinheim, **2000**, Chapter 12.

[26] E. Gorecka, D. Pociecha, J. Mieczkowski, J. Matraszek, D. Guillon, B. Donnio, *J. Am. Chem. Soc.* **2004**, *126*, 15946–15947.

[27] V. S. K. Balagurusamy, G. Ungar, V. Percec, G. Johansson, *J. Am. Chem. Soc.* **1997**, *119*, 1539–1555.

[28] J. Boersma, *J. Chem. Phys.* **1981**, *74*, 6989–6990.

[29] a) A. Lohr, M. Lysetska, F. Würthner, *Angew. Chem.* **2005**, *117*, 5199–5202; *Angew. Chem. Int. Ed.* **2005**, *44*, 5071–5074; b) H. Engelkamp, S. Middelbeek, R. J. M. Nolte, *Science* **1999**, *284*, 785–788; c) N. A. J. M. Sommerdijk, P. J. J. A. Buynsters, H. Akdemir, D. G. Geurts, M. C. Feiters, R. J. M. Nolte, B. Zwanenburg, *Chem. Eur. J.* **1998**, *4*, 127–136.

Received: July 14, 2007
Published online: October 1, 2007

